



**Michigan  
Technological  
University**

Michigan Technological University

Digital Commons @ Michigan Tech

---

Department of Biomedical Engineering  
Publications

Department of Biomedical Engineering

2-21-2019

## Polydopamine and collagen coated micro-grated polydimethylsiloxane for human mesenchymal stem cell culture

Dhavan Sharma

*Michigan Technological University*

Wenkai Jia

*Michigan Technological University*

Fei Long

*Michigan Technological University*

Shweta Pati

*Michigan Technological University*

Qing-Hui Chen

*Michigan Technological University*

*See next page for additional authors*

Follow this and additional works at: <https://digitalcommons.mtu.edu/biomedical-fp>



Part of the [Engineering Commons](#)

---

### Recommended Citation

Sharma, D., Jia, W., Long, F., Pati, S., Chen, Q., Qyang, Y., Lee, B. P., Choi, C. K., & Zhao, F. (2019). Polydopamine and collagen coated micro-grated polydimethylsiloxane for human mesenchymal stem cell culture. *Bioactive Materials*, 4, 142-150. <http://dx.doi.org/10.1016/j.bioactmat.2019.02.002>  
Retrieved from: <https://digitalcommons.mtu.edu/biomedical-fp/43>

Follow this and additional works at: <https://digitalcommons.mtu.edu/biomedical-fp>



Part of the [Engineering Commons](#)

---

## Authors

Dhavan Sharma, Wenkai Jia, Fei Long, Shweta Pati, Qing-Hui Chen, Yibing Qyang, Bruce P. Lee, Chang Kyoung Choi, and Feng Zhao



# Polydopamine and collagen coated micro-grated polydimethylsiloxane for human mesenchymal stem cell culture

Dhavan Sharma<sup>a</sup>, Wenkai Jia<sup>a</sup>, Fei Long<sup>b</sup>, Shweta Pati<sup>a</sup>, Qinghui Chen<sup>c</sup>, Yibing Qyang<sup>d</sup>, Bruce Lee<sup>a</sup>, Chang Kyong Choi<sup>a,b</sup>, Feng Zhao<sup>a,\*</sup>

<sup>a</sup> Department of Biomedical Engineering, Michigan Technological University, 1400 Townsend Drive, Houghton, MI, 49931, USA

<sup>b</sup> Department of Mechanical Engineering-Engineering Mechanics, Michigan Technological University, 1400 Townsend Drive, Houghton, MI, 49931, USA

<sup>c</sup> Department of Kinesiology and Integrative Physiology, Department of Kinesiology and Integrative Physiology, Houghton, MI, 49931, USA

<sup>d</sup> Yale Stem Cell Center, Yale University School of Medicine, 300 George Street, New Haven, CT 06511, USA

## ARTICLE INFO

### Keywords:

Polydimethylsiloxane

Polydopamine

Collagen

Micro-grating

Human mesenchymal stem cell

## ABSTRACT

Natural tissues contain highly organized cellular architecture. One of the major challenges in tissue engineering is to develop engineered tissue constructs that promote cellular growth in physiological directionality. To address this issue, micro-patterned polydimethylsiloxane (PDMS) substrates have been widely used in cell sheet engineering due to their low microfabrication cost, higher stability, excellent biocompatibility, and most importantly, ability to guide cellular growth and patterning. However, the current methods for PDMS surface modification either require a complicated procedure or generate a non-uniform surface coating, leading to the production of poor-quality cell layers. A simple and efficient surface coating method is critically needed to improve the uniformity and quality of the generated cell layers. Herein, a fast, simple and inexpensive surface coating method was analyzed for its ability to uniformly coat polydopamine (PD) with or without collagen on micro-grated PDMS substrates without altering essential surface topographical features. Topographical feature, stiffness and cytotoxicity of these PD and/or collagen based surface coatings were further analyzed. Results showed that the PD-based coating method facilitated aligned and uniform cell growth, therefore holds great promise for cell sheet engineering as well as completely biological tissue biomanufacturing.

## 1. Introduction

Scaffold designing is one of the significant challenges in fabrication of engineered tissue constructs. Results from high-resolution microscopy and image processing have revealed that cellular and extra-cellular matrix (ECM) components of native tissues are organized in precise architectural order [1–6]. To mimic the natural tissue structure, directional scaffolding materials have been developed to guide cellular growth and ECM deposition. As an another approach, scaffold-free and aligned cell sheets have also been developed, which can be stacked layer by layer to fabricate three-dimensional (3D) completely biological and anisotropic tissues [7]. Controlled cellular organization in a specific direction has became increasingly crucial to develop tissue-engineered vascular grafts [8], cardiac patch [9], and nerve regenerative scaffolds [10]. Micro-topography controlled cellular behavior has been widely examined by researchers in the past few years. For example, Rim et al. used aligned microgrooves with 5 µm height and 30 µm width to

develop aligned vascular smooth muscle cell sheets, which can further be used as building blocks to fabricate tissue-engineered vascular patches [11]. In another study, aligned microgroove and micro-wavy surface with 5 µm groove height and 20 µm width showed enhanced EC alignment and adhesion [12]. These topographical features are crucial to promote desired cellular alignment and adhesion in 3D complex tissues.

Polydimethylsiloxane (PDMS) has been widely used to create nano- or micron-scale features for surface topography associated studies due to its high stability, excellent biocompatibility and low fabrication cost [13,14]. PDMS is highly hydrophobic and therefore, requires surface modification to enhance cellular adhesion. Oxygen plasma etching followed by collagen adsorption has been applied to promote cellular attachment and proliferation on the PDMS substrates [15,16]. Nevertheless, this method is dependent on the weak electrostatic and van der Waals interaction between PDMS and collagen, resulting in an unstable collagen coating. We have recently published a layer-by-layer

Peer review under responsibility of KeAi Communications Co., Ltd.

\* Corresponding author.

E-mail address: [fengzhao@mtu.edu](mailto:fengzhao@mtu.edu) (F. Zhao).

grafting method to develop uniform human mesenchymal stem cell (hMSC) sheets on the PDMS substrates [17]. In this approach, PDMS was treated by oxygen plasma to convert silane ( $\text{Si}-\text{CH}_3$ ) into silanol ( $\text{Si}-\text{OH}$ ) groups. Subsequently, the silanol groups were grafted with (3-aminopropyl) triethoxy silane (APTES), followed by collagen I cross-linking via glutaraldehyde [17]. Although highly effective, this method is complex, time-consuming, and requires oxygen plasma pretreatment. It has been reported that resulting silanol groups after oxygen plasma could condense with their neighboring groups to form a brittle  $\text{SiO}_x$  layer on the PDMS surface [18]. Oxygen plasma even for 60–120 s can densify  $\text{SiO}_x$  layer, increasing tensile force buildup and resulting in crack formation, which can alter both topographical and mechanical properties of the PDMS surface [18]. A study done by Yang et al. showed that oxygen plasma exposure just for 30 s could create cracks on the PDMS surface [19]. Alteration in these surface properties can significantly influence cellular orientation, migration and phenotypic expression. Therefore, it is not advisable to use oxygen plasma for PDMS surface treatment, especially for those that have nano or micron scale topographical features on the surface.

Alternatively, mussel-inspired polydopamine (PD) can virtually form a coating on all types of materials including metals, semiconductors, ceramics and synthetic polymers by covalent bonding or non-covalent strong interfacial interactions such as hydrogen bonds,  $\pi$ - $\pi$  electron interaction and cation- $\pi$  interactions [20,21]. PD coating has also been applied on PDMS substrates for conjugating biomolecules to upgrade its performance for cell adhesion and other applications [22–24]. The strong adhesive nature of polydopamine is attributed to the presence of biomimetic catechol and primary amines that are found in the chemical structure of the native mussel adhesive proteins [20]. Although promising, the PD-based surface coating can raise few concerns while applied on micro-patterned PDMS substrates. During the polymerization process from dopamine monomers to PD, the covalent and non-covalent interaction in the reaction system can form supramolecular aggregates [25]. It is possible that these supramolecular aggregates formed between microgrooves can alter the overall surface topography of the PDMS substrates, which could in turn affect not only the cell layer quality but also the cellular phenotypic expression. Therefore, in this study, micro-grated PDMS substrates were coated with collagen (PDMS/collagen), PD (PDMS/PD), and PD and collagen (PDMS/PD/collagen) to compare the surface topography, hydrophilicity, surface stiffness and cell coverage after different surface coatings.

Human mesenchymal stem cell (hMSCs) are multipotent and can stimulate tissue regeneration by paracrine effects [26]. Their therapeutic potential has been proved in diverse tissue engineering applications such as wound healing [27], bone regeneration [28], small diameter vascular graft fabrication [29–31], and cardiac repair [32]. Moreover, previous studies have shown that physiologically low (2%) oxygen preserves the stemness and paracrine effects of hMSCs [33–35]. Therefore, in this study, hMSCs were selected as model cells to further examine their cellular response toward PD based surface coatings under the physiological hypoxic environment.

## 2. Materials and methods

### 2.1. PDMS substrate fabrication and surface coating

The micro-gratings were created by using electron beam lithography on the poly(methyl methacrylate)-coated silicon wafer [36]. The aligned micron scale gratings were created with 5  $\mu\text{m}$  of grating depth, 15  $\mu\text{m}$  grating width and 30  $\mu\text{m}$  of grating pitch. PDMS casts were prepared from silicon wafer mold using SYLGARD 184 Silicone Elastomer Kit (Dow-corning, Midland MI) under manufacturer's instruction. Briefly, the mixture was poured onto a silicon wafer, degassed, and cured at 65 °C for 4 h to transfer the pattern. Plastic petri dishes (Fisher scientific, Hampton, NH) were used as a mold to cast flat

homogenous PDMS substrates. PDMS substrates were punched in circular disks with 1.19 cm of diameter. PDMS substrates were cleaned and sterilized under UV light. For collagen coating (PDMS/collagen), PDMS substrates were immersed in 20  $\mu\text{g}/\text{mL}$  bovine collagen (Sigma Aldrich, St. Louis, MO) solution (prepared in 0.01 M HCl) for 2 h at room temperature. PD and PD/collagen coatings were developed on PDMS substrates as described by Chuah et al. in their study [37]. Briefly, to develop a PD coating on PDMS surface (PDMS/PD), PDMS was immersed in 0.01% W/V 3-hydroxytyramine hydrochloride (Dopamine-HCl) (ACROS Organics, Fisher scientific) solution prepared in 10 mM Tris-HCl (pH 8.5) for 24 h and rinsed twice with DI water to remove unattached PD molecules. For PD and collagen coating (PDMS/PD/collagen), PD coated PDMS were first air dried under the hood and subsequently immersed in 20  $\mu\text{g}/\text{mL}$  bovine collagen (Sigma Aldrich) solution for 2 h. After different surface coatings, all PDMS substrates were air dried and incubated overnight under alpha-minimal essential medium ( $\alpha$ -MEM) at 37 °C in CO<sub>2</sub> incubator. Micro-grated PDMS substrates are mentioned as aligned PDMS for convenience in describing result images and graphs.

### 2.2. FTIR analysis

Chemical composition of flat and aligned PDMS with different surface coatings was analyzed using fourier transform infrared spectroscopy (FTIR) with attenuated total reflectance (ATR) mode. Spectra of pristine PDMS as well as PDMS/collagen, PDMS/PD, and PDMS/PD/collagen were obtained to investigate chemical composition of the surface coatings. PDMS samples were prepared freshly and air-dried before the FTIR analysis. The spectra were recorded between 700 and 3700  $\text{cm}^{-1}$  range at room temperature (RT) using FTIR-ATR spectrometer (Perkin-Elmer, Waltham, MA).

### 2.3. Surface topography and elastic modulus characterization

All atomic force microscopy (AFM) experiments were carried out with a Dimension ICON AFM system (Bruker, USA). Peak force tapping mode was applied for all the nano-mechanical measurements and topography characterization. SNL-C cantilevers (Bruker, USA) were used in all of the experiments. The spring constant was calibrated using Sader's method [38] before each experiment, and the calibrated values were  $0.2 \pm 0.11 \text{ N/m}$ . For each sample, 4 various positions were scanned by the AFM in order to check the uniformity. The average values of both surface roughness and elastic modulus of the 4 various positions were reported. NanoScope Analysis v1.40 software (Bruker, USA) was used for all AFM data analysis.

### 2.4. Surface hydrophilicity characterization

Water drop contact angle measurement was performed to analyze surface hydrophilicity using G10 contact angle measurement system (Krüss, Germany). In each group, the hydrophilicity of four different samples was analyzed by static sessile drop method. On each sample, at least five different areas were selected to measure the contact angle of water droplets on the surface.

### 2.5. hMSC culture and cell coverage measurement

Bone marrow derived hMSCs were obtained from Texas A&M University Health Sciences Center. hMSCs (passage 4) were seeded on the PDMS substrates with seeding density of 10,000 cells/cm<sup>2</sup> and cultured under physiological hypoxic (2% O<sub>2</sub>) environment with complete  $\alpha$ -MEM containing 20% Fetal bovine serum (FBS), 1% L-glutamine (Thermo Fisher Scientific, Waltham, MA) and 1% penicillin/streptomycin (Thermo Fisher Scientific). In order to measure hMSC coverage on different surfaces, cells were stained by immunofluorescent antibody against F-actin. At days 3, 6, and 9, cells were fixed with

formaldehyde and stained with Rhodamine Phalloidin (R415, Invitrogen, Carlsbad, CA) and 4',6-diamidino-2-phenylindole (DAPI) (Sigma Aldrich) to observe cytoskeletal F-actin and cell nuclei respectively, under an Olympus FV1000 (Olympus Corporation, Shinjuku, Japan) fluorescence microscope. Cell coverage was determined by calculating percentage area covered by hMSCs using default color thresholding function in Image J software.

## 2.6. Cytotoxicity measurements

LIVE/DEAD Viability/Cytotoxicity Kit (Invitrogen) was used to differentiate live and dead hMSCs cultured on different surfaces at days 3, 6 and 9. hMSCs cultured on different PDMS coatings were washed twice with sterile phosphate buffer saline (PBS) and stained with Calcein AM (2 µM) and Ethidium Homodimer-1 (EthD-1) (4 µM) solution prepared in sterile PBS for 30 min at room temperature. Samples were mounted on the coverslip using sterile PBS and observed under fluorescence microscope with red [ex/em ~495 nm/~635 nm] and green [ex/em ~495 nm/~515 nm] filters to observe dead and live cells respectively, under an Olympus FV1000 (Olympus Corporation) fluorescence microscope.

## 2.7. Statistical analysis

All statistical results were obtained from triplicated experiments. In software-based image analysis, four non-overlapping panels were randomly selected and analyzed from each sample to perform unbiased statistical analysis. The results were reported as mean  $\pm$  standard deviation. Statistical comparisons between experimental groups were performed by one-way ANOVA and Tukey's post hoc test using RStudio 1.1.456 software. Result graphs were plotted with GraphPad Prism 6 software. Results were considered statistically significant for \* $p < 0.05$ , \*\* $p < 0.01$ , \*\*\* $p < 0.001$ , \*\*\*\* $p < 0.0001$ .

## 3. Results

### 3.1. Characterization of PDMS surface topography and chemical composition

Surface features of micro-grated and flat PDMS substrates were characterized using AFM (Fig. 1). The micro-gratings were successfully transferred from the silicon wafer to the PDMS substrates. The grating depth, width and pitch on PDMS casts were measured as 5 µm, 15 µm and 30 µm, respectively (Fig. 1 B, C). In contrast, the PDMS casted from flat petri dish molds had a smooth surface as shown in Fig. 1A. The stages of dopamine polymerization into PD and the possible covalent as well as non-covalent interactions between PD and collagen are illustrated in Fig. 1D. Oxidation of dopamine under alkaline TRIS buffer forms dopamine-quinone that undergoes intramolecular cyclization to form 5,6-dihydroxyindole, which further undergoes polymerization to form polydopamine [39]. Upon collagen coating on the PD layer, catechol present in the PD structure forms covalent as well as non-covalent interactions such hydrogen bonds,  $\pi$ - $\pi$  electron interaction and cation-  $\pi$  interaction with collagen [21,40,41] (Fig. 1D).

The surface coatings on aligned and flat PDMS substrates were analyzed by FTIR spectra (Fig. 2). The transformations around 1255, 1013, 793 cm<sup>-1</sup> denoted the stretching of Si-CH<sub>3</sub>, Si-O-Si, Si-CH<sub>3</sub> groups, which are specific for PDMS [42]. In PDMS/collagen samples, collagen specific peptide bond (-CO-NH-) was detected by FTIR spectra. Secondary amine(-NH) of this peptide bond was characterized by absorption band between 3350 cm<sup>-1</sup> to 3087 cm<sup>-1</sup>, mainly ascribed to the stretching vibrations of N-H group [43]. The PDMS/PD and PDMS/PD/collagen samples also exhibited broad absorption band at 3400 cm<sup>-1</sup>, due to the presence of PD specific stretching vibration of N-H and O-H groups [44,45]. Since PD and collagen both shows absorption in the range of 3000 cm<sup>-1</sup> -3400 cm<sup>-1</sup> due to the presence of N-H

group, C=O specific stretching vibration was further analyzed, which is exclusive for collagen and absent in PD. Both, PDMS/collagen as well as PDMS/PD/collagen samples showed distinctive peak at 1640 cm<sup>-1</sup>, which is ascribed to the collagen specific stretching vibration of C=O bond [41]. Pristine PDMS and PDMS/PD samples did not show any absorbance at 1640 cm<sup>-1</sup>, validating absence of collagen. Absorption band at 2850 cm<sup>-1</sup> further indicated presence of PD specific catechol-OH [46] in PDMS/PD, but not in PDMS/PD/collagen samples (Fig. 2).

### 3.2. Characterization surface roughness, elastic modulus and hydrophilicity

The surface roughness as well as overall surface topography of micro-grated and flat PDMS substrates after different coatings were analyzed using AFM, and compared with pristine PDMS samples. The height, width and pitch of the microgrooves were measured to confirm preservation of overall surface topography after respective surface coatings. As indicated in Fig. 3C, all three of the surface coatings formed a uniform layer without severely altering overall micron scale surface topography. There were no significant differences in surface roughness between pristine PDMS, PDMS/collagen and PDMS/PD samples, in both aligned and flat groups. However, in aligned groups, PDMS/PD/collagen showed significantly reduced roughness ( $3.17 \pm 0.38$  nm) compared to PDMS/PD ( $5.25 \pm 0.18$  nm) ( $p < 0.001$ ) as well as pristine PDMS ( $4.75 \pm 0.29$  nm) ( $p < 0.05$ ) (Fig. 3B). Similarly, in flat groups, PDMS/PD/collagen showed significantly reduced roughness ( $3.46 \pm 0.30$  nm) compared to PDMS/PD ( $4.93 \pm 0.47$  nm) ( $p < 0.05$ ) and pristine PDMS ( $5.38 \pm 0.10$  nm) ( $p < 0.01$ ) as indicated in Fig. 2B.

The surface elastic moduli after different surface coatings were analyzed using AFM. Aligned and flat PDMS coated with collagen, PD and PD/collagen had increased surface stiffness compared to pristine PDMS as indicated in Fig. 4A and B. Moreover, it was observed that aligned as well as flat PDMS/PD [ $6.59 \pm 0.23$  MPa (aligned);  $6.56 \pm 0.70$  MPa (flat)] and PDMS/PD/collagen [ $8.93 \pm 0.29$  MPa (aligned);  $11.91 \pm 0.90$  MPa (Flat)] samples had significantly increased surface stiffness compared to pristine PDMS substrates [ $1.72 \pm 0.11$  MPa (aligned);  $2.20 \pm 0.05$  MPa (Flat)] ( $p < 0.0001$ ). Similarly, aligned PDMS/PD and PDMS/PD/collagen groups showed significantly increased surface stiffness compared to PDMS/collagen substrates ( $3.08 \pm 0.16$  MPa,  $p < 0.01$ ).

It is well known that collagen grafting reduces surface hydrophobicity of pristine PDMS [17]. Surface hydrophilicity of PDMS, PDMS/collagen, PDMS/PD and PDMS/PD/collagen coatings in both aligned and flat groups was measured using water drop contact angle measurement (Fig. 5A). PDMS/collagen, PDMS/PD and PDMS/PD/collagen groups showed significant reduction ( $p < 0.0001$ ) in contact angle compared to uncoated samples, in both aligned and flat groups (Fig. 5B). Both aligned and flat PDMS/PD/collagen coatings (Aligned:  $50.43 \pm 1.12^\circ$ ; Flat:  $76.55 \pm 0.52^\circ$  showed significant reduction ( $p < 0.0001$ ) in the contact angle compared to PDMS/collagen (Aligned:  $94.35 \pm 0.39^\circ$ ; Flat:  $91.96 \pm 0.38^\circ$ ) and PDMS/PD surfaces (Aligned:  $88.55 \pm 0.61^\circ$ ; Flat:  $81.95 \pm 0.43^\circ$ ) (Fig. 5B). These water drop contact angle measurements were comparable to the previously published contact angle values of PD coated PDMS substrates [47]. After PDMS/PD/collagen coating, aligned PDMS showed significant reduction in contact angle compared to flat PDMS substrates ( $p < 0.0001$ ) (Fig. 5B).

### 3.3. hMSC coverage and cytotoxicity measurement

hMSCs were grown on flat and aligned PDMS substrates under physiological hypoxic (2% O<sub>2</sub>) environment for 9 days. The cytoskeleton and cell nuclei were stained to observe their coverage and alignment (Fig. 6A and B). hMSCs cultured on both aligned and flat substrates exhibited significantly increased cell coverage on PDMS/PD as well as PDMS/PD/collagen groups compared to untreated PDMS

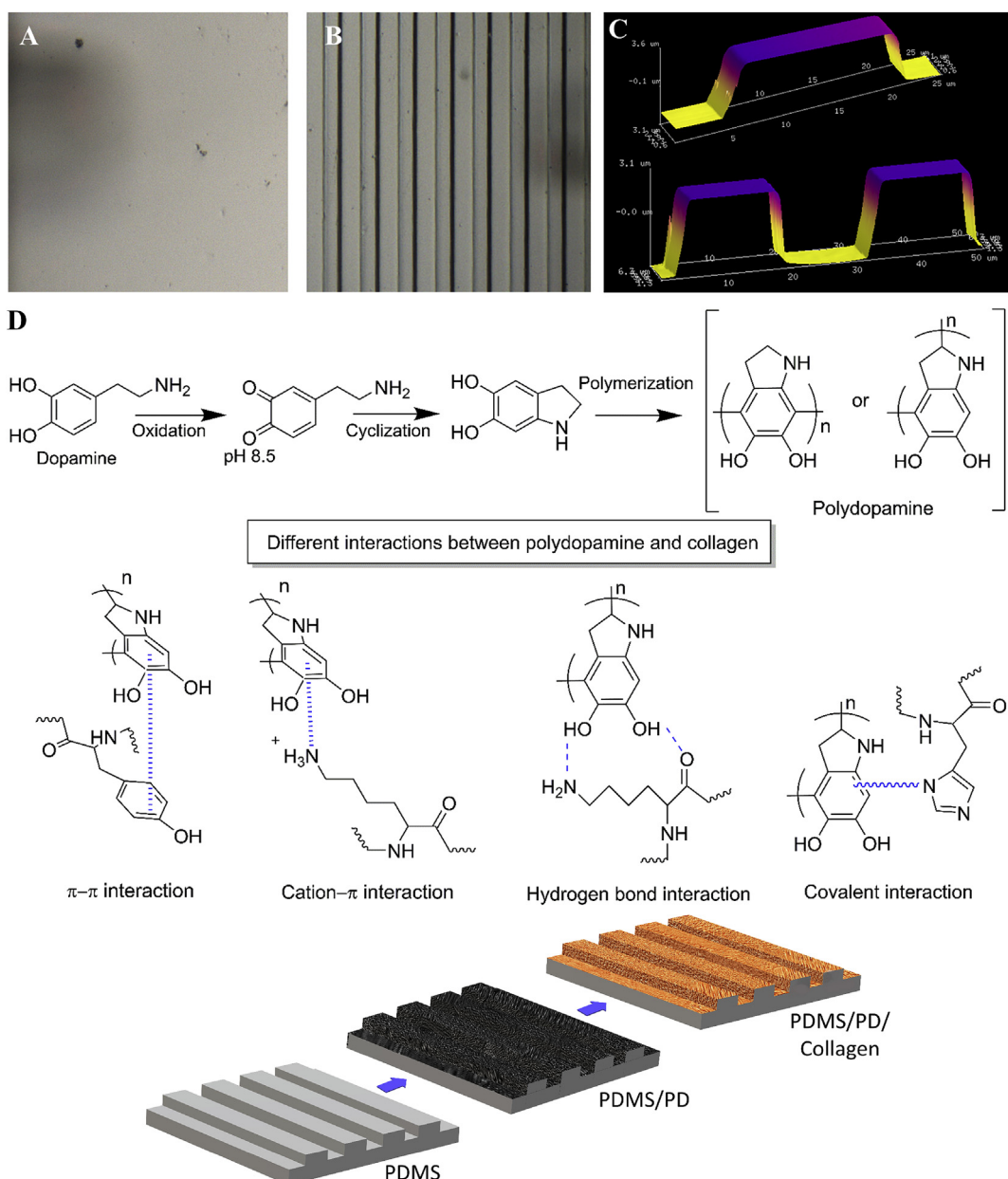


**Fig. 1.** Surface topographical feature of PDMS substrates characterized by AFM. (A) Flat PDMS, (B) PDMS with micro-gratings, (C) Analysis of grating depth (5  $\mu\text{m}$ ), width (15  $\mu\text{m}$ ) and pitch (30  $\mu\text{m}$ ) using NanoScope analysis software v1.40. The micro-gratings were successfully transferred from silicon wafer mold to PDMS. (D) Schematic representation of dopamine polymerization and different possible chemical interactions between PD and collagen.

substrates ( $p < 0.0001$ ) (Fig. 6C). Within PDMS/PD and PDMS/PD/collagen groups, hMSCs showed significantly increased cell coverage on flat substrates ( $p < 0.0001$  and  $< 0.05$ , respectively) compared to aligned samples on day 3 (Fig. 6C). On day 6, hMSCs cultured on both PDMS/PD and PDMS/PD/collagen showed significantly increased cell coverage compared to PDMS ( $p < 0.0001$ ) as well as PDMS/collagen ( $p < 0.01$ ) substrates (Fig. 6D). Within PDMS/collagen group, hMSCs cultured on flat substrates showed significantly increased cell coverage ( $p < 0.01$ ) compared to aligned substrates (Fig. 6D). On day 9, similar cell coverage phenomenon was observed as day 6. hMSCs cultured on both PDMS/PD and PDMS/PD/collagen showed significantly increased cell coverage compared to PDMS ( $p < 0.0001$ ) as well as PDMS/collagen ( $p < 0.0001$ ) substrates (Fig. 6E). No significant difference in cell coverage was observed between aligned and flat samples of PDMS and PDMS/collagen group on day 9 (Fig. 6E). hMSCs cultured on pristine PDMS and only collagen aligned as well as flat substrates

showed gradual decrease in cell coverage from day 3 to day 9 (Fig. 6). While hMSCs cultured on PDMS/PD and PDMS/PD/collagen substrates showed increased coverage with complete confluence from day 3 to day 9 (Fig. 6). In addition, hMSCs cultured on aligned substrates, especially PD and PD/collagen coated aligned PDMS showed highly aligned and organized actin cytoskeleton in the direction of microgrooves (Fig. 6A).

In order to analyze cytotoxicity of different PDMS surface coatings, Live/Dead staining was performed. Live cells stained by calcein AM were observed as green fluorescence signal and dead cells were observed as red fluorescence generated by EthD-1 due to compromised plasma membrane integrity (Fig. 7). It was observed that PDMS coated with collagen, PD and PD/collagen showed negligible dead cell signals. In addition, calcein AM staining further verified highly aligned and uniform hMSCs culture on the aligned PDMS/PD and PDMS/PD/collagen samples compared to all other groups (Fig. 7). The data obtained from this study authenticated non-cytotoxic effects of PD and PD/

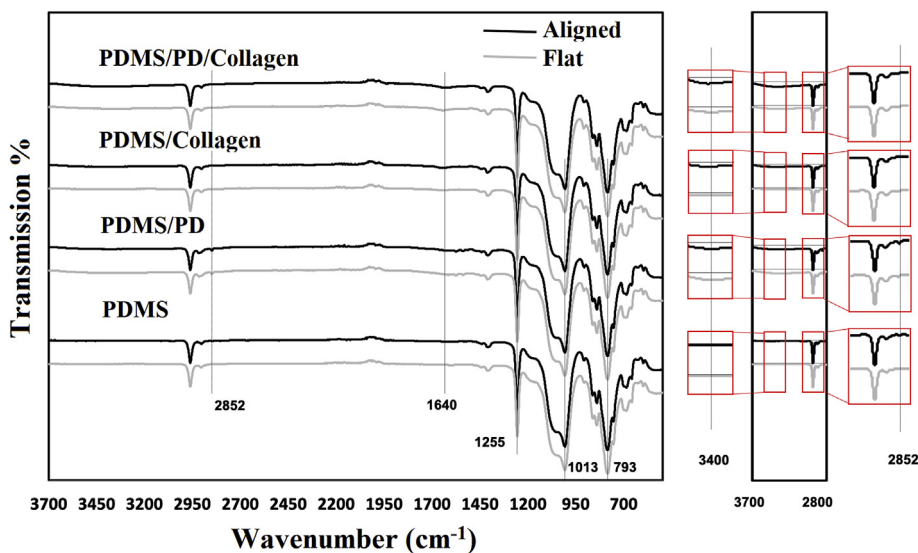


**Fig. 2.** FTIR-ATR spectra of aligned and flat PDMS with different surface coatings in the range of 3700  $\text{cm}^{-1}$  to 700  $\text{cm}^{-1}$ . PD and collagen specific peaks have been emphasized to validate the presence of PD and/or collagen specific functional groups.

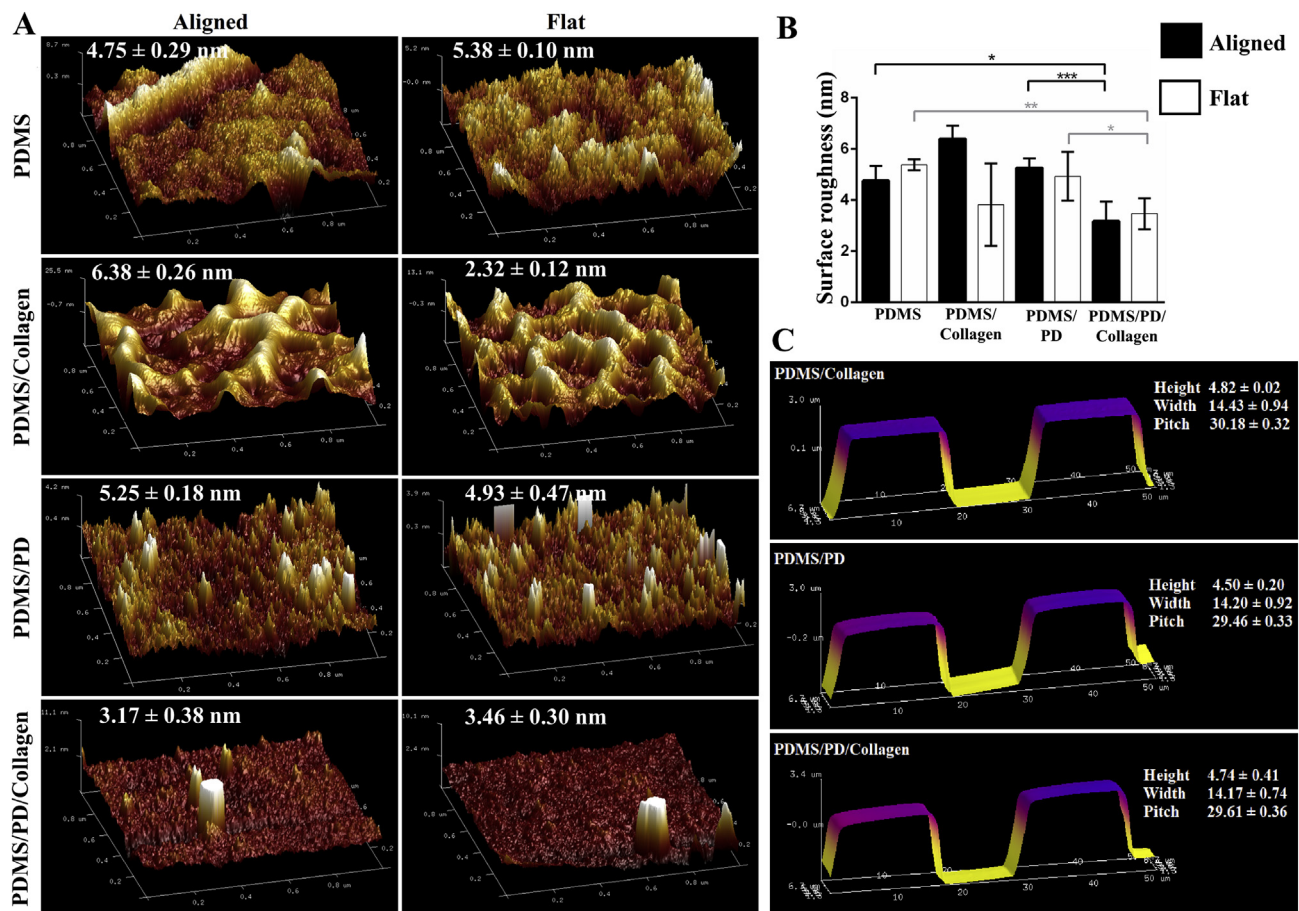


**Fig. 3.** Surface roughness analysis. (A) Surface roughness characterized as an average deviation measured by cantilever in tapping mode AFM for aligned and flat PDMS substrates with different surface coatings. (B) Quantitative representation of surface roughness in nanometer (nm). (C) Characterization of overall surface topographical features of aligned PDMS substrates after different surface coatings. The PDMS/PD/collagen surface coating showed significantly reduced surface roughness compared to all other groups.

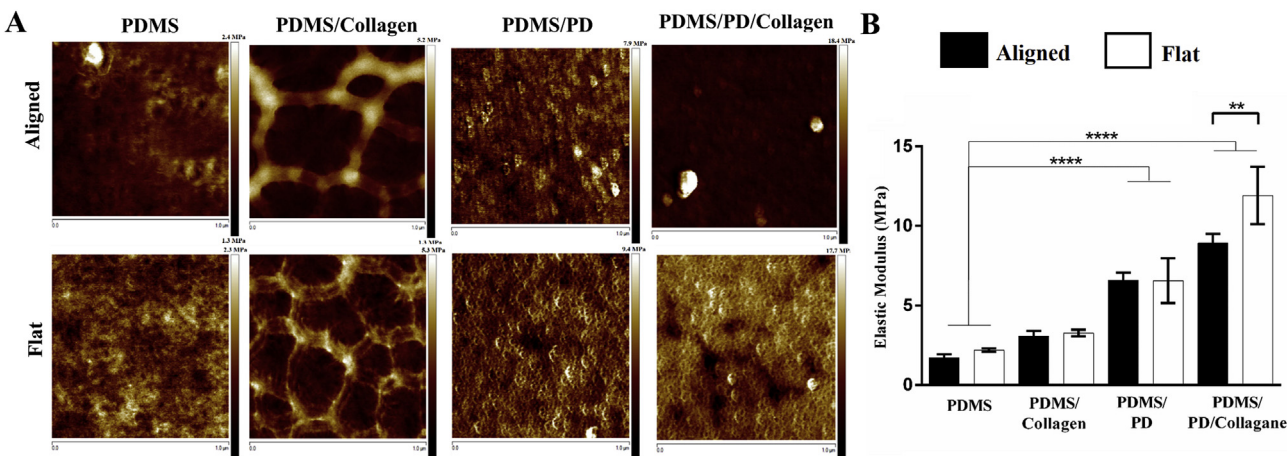


**Fig. 4.** Characterization of surface stiffness after different surface coatings. (A) Elastic modulus measurement by AFM analysis. (B) Comparison of surface stiffness on different surface coatings by NanoScope Analysis software. PD and PD/collagen coating significantly increased surface elastic moduli compared to pristine PDMS substrates.

collagen based coatings on hMSCs especially during physiological hypoxic culture environment.

#### 4. Discussion

In this study, PD based surface coatings were analyzed in order to achieve a simple, cost effective and oxygen plasma-independent surface treatment for micro-grated PDMS substrates. Under alkaline condition, dopamine monomers polymerize into polydopamine (PD) and form a thin film on the PDMS surface due to strong intermolecular non-covalent interactions between PD and PDMS [25,37]. Moreover, to enhance appropriate cellular attachment by providing native cell adhesion peptides, collagen coating was also applied on PD treated PDMS substrates.

The PD and PD/collagen were successfully coated on both flat and micro-grated PDMS surfaces, as indicated by the FTIR spectra, which showed both PD-specific stretching vibrations of N-H, -OH and methylene groups as well as the collagen-specific stretching vibrations of N-H and C=O groups (Fig. 2). Direct surface adsorption of collagen on PDMS can form a polygonal structure containing strands of collagen fibrils, which is caused by hydrogen bond interaction between repeatedly placed hydroxyproline, proline and glycine that organizes polymer chains into a tight triple helix [49]. Similar polygonal structure of collagen I fibrils was observed on both aligned and flat PDMS/collagen substrates (Fig. 3A). However, multiple interactions such as

hydrogen bonds [48], cation- $\pi$  interaction,  $\pi$ - $\pi$  interaction and covariant bonds between catechol -OH groups of PD and collagen [21,40] can disrupt the self-assembly of collagen fibrils due to their strong crosslinking with PD as well as the reduction in intramolecular hydrogen bonding within collagen fibrils. As a result, collagen specific polygonal structure was not observed on PDMS/PD/collagen samples (Fig. 3A). Evidently, only PD but not PD/collagen coating, showed catechol -OH specific absorption band at 2850 cm<sup>-1</sup> (Fig. 2), indicating engagement of catechol-OH in chemical bonding with the collagen. One of the concerns with PD coating was formation of supramolecular aggregates, which might alter or overcome the surface topography. AFM scanning displayed that PD coating had preserved the features of microgrooves without severely altering their original size parameters (Fig. 3C). A previous study using the same PD coating method on PDMS has revealed that the PD layer had a thickness of  $40 \pm 10$  nm [50]. It is due to this nano scale thickness of PD layer, the micron-scale surface topography was preserved after the PD-based coatings. Previous studies have also shown that PD and PD/collagen coating can significantly reduce surface hydrophobicity of flat PDMS substrates [37,47]. In the current study, both PDMS/PD and PDMS/PD/collagen coatings significantly improved the surface hydrophilicity of micro-grated and flat PDMS substrates compared to pristine PDMS as well as PDMS/collagen samples. Moreover, after PD/collagen coating, surface hydrophobicity of micro-grated PDMS was significantly reduced compared to flat substrates (Fig. 5B). The air trapped between micro-grooves, along with

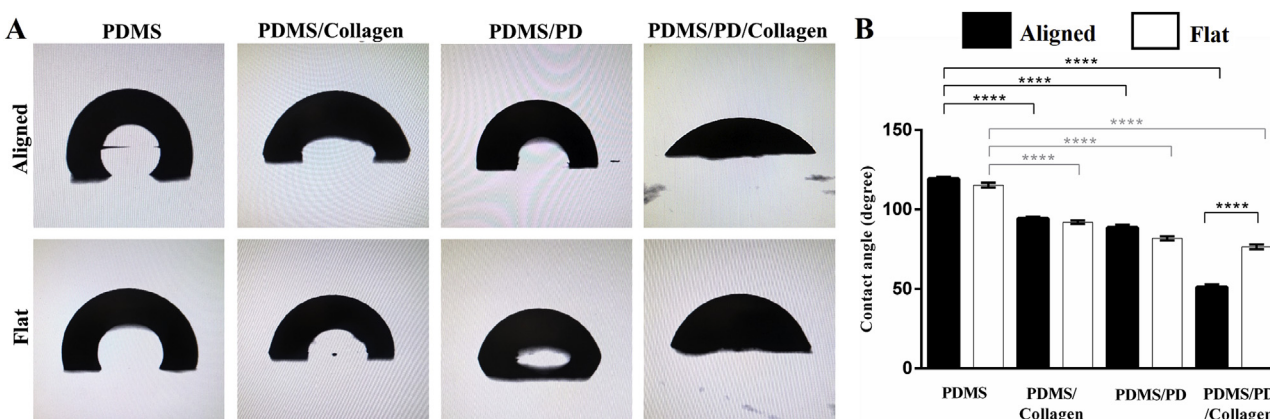


**Fig. 5.** Surface hydrophilicity analysis. (A) Representative images of water droplet formation on aligned and flat PDMS substrates with different coatings. (B) Quantification of water drop contact angle. Collagen, PD and PD/collagen coating significantly improved surface hydrophilicity, with highest hydrophilicity observed after PDMS/PD/collagen coating.

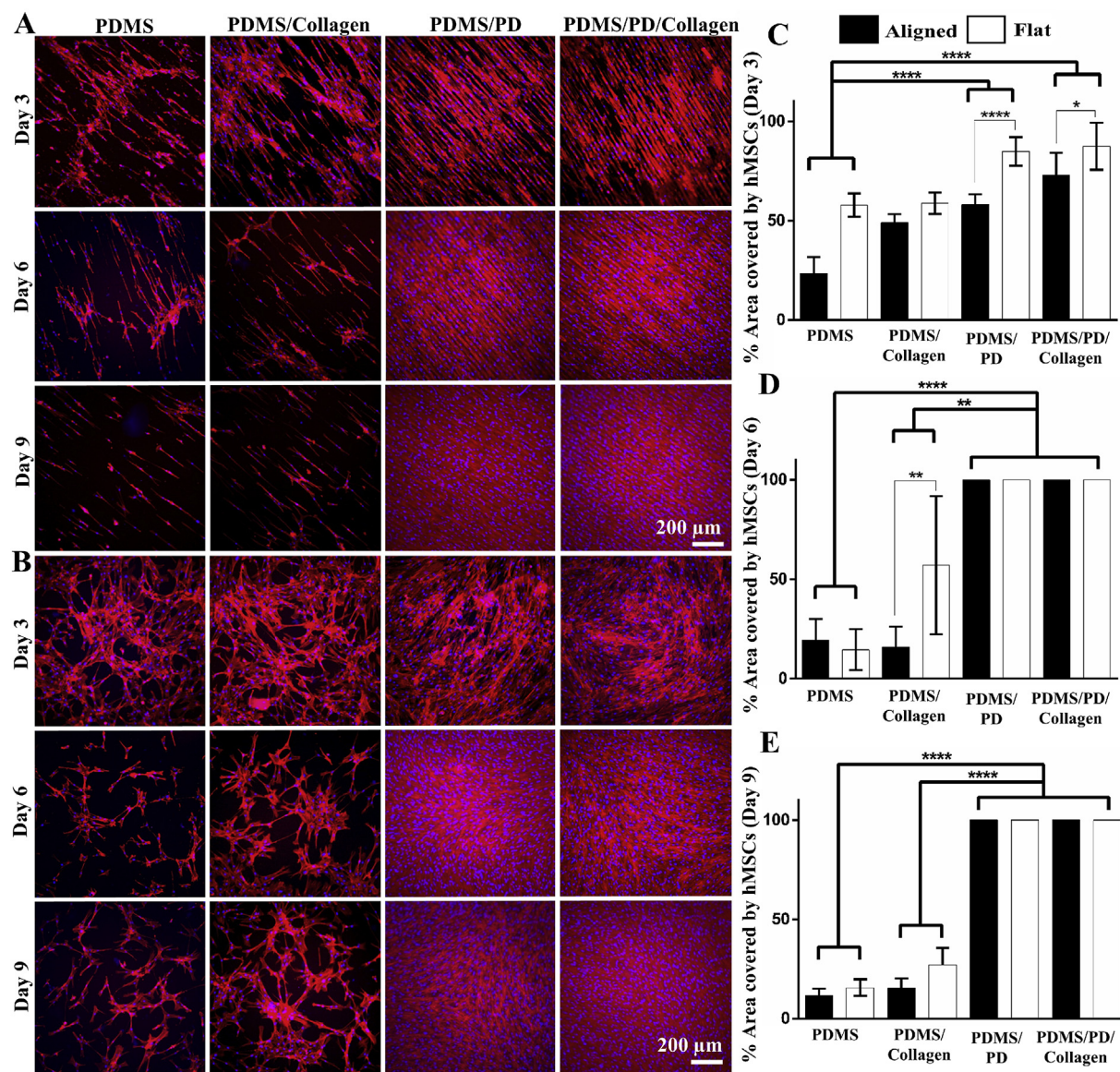


**Fig. 6. Measurement hMSC coverage.** hMSC cultured on (A) aligned and (B) flat PDMS substrates with different surface coatings under hypoxic (2% O<sub>2</sub>) environment. Cytoskeleton and cell nuclei were observed by F-actin (red) and DAPI (blue) staining, respectively. Quantification of percentage area covered by hMSCs on (C) day 3, (D) day 6 and (E) day 9 using ImageJ software. PDMS/PD and PDMS/PD/collagen samples showed significantly increased hMSC coverage compared to other groups.

surface hydrophobicity affects contact angle and the shape of water droplet [51]. With significantly improved hydrophilicity after PD/collagen coating, the air that was trapped between the grooves was replaced by water, which resulted in significant reduction of water-drop contact angle (Fig. 5B).

Surface stiffness can be altered by different surface coatings. PDMS/collagen coating via simple adsorption showed significantly lower elastic modulus compared to PD and PD/collagen coatings (Fig. 4B). Moreover, during PDMS/collagen surface coating, weaker interactions between collagen and PDMS might pose risk of collagen leaching into the cell culture medium. The cell coverage measurement indicated that both aligned and flat PDMS/collagen substrates showed gradual decrease in hMSC coverage area from day 3 to day 9 (Fig. 6). These results indicated instability of collagen coating on the PDMS substrates, which might have resulted in hMSC detachment. It has been shown that PD coating can significantly increase surface stiffness of synthetic polymers [52] because PD itself has modulus of around 10 GPa [53]. Similarly, in current study, PD coating significantly increased surface moduli of PDMS/PD and PDMS/PD/collagen substrates compared to pristine

PDMS (Fig. 4). It has been reported that hMSCs initial attachment and growth was linearly increased with increase in substrate stiffness in the range of 5–22 MPa [54,55]. We also observed similar linear correlation between hMSC coverage and surface elastic moduli in the range of ~1.7–12.0 MPa (Figs. 4 and 6).

Surface gratings can significantly promote cellular alignment as well as adhesion [12,56,57], which has been attributed to the topographical feature directed focal adhesion complex formation and cytoskeletal reorganization [58]. Regardless of surface coatings, the micro-gratings successfully regulated hMSCs alignment, which was qualitatively observed by organization of F-actin cytoskeleton (Fig. 6A). However, during the first three days of culture it was observed that hMSCs showed higher coverage on flat substrates compared to aligned substrates (Fig. 6C). It might be possible that on micro-grated substrates, hMSCs' initial coverage rate might have reduced due to focal adhesion complex formation and cytoskeleton reorganization in the direction of the micro grooves. However, on day 3 onwards, no significant difference in hMSCs coverage was observed between aligned and flat substrates, especially with PD and PD/collagen coatings (Fig. 6D and E).

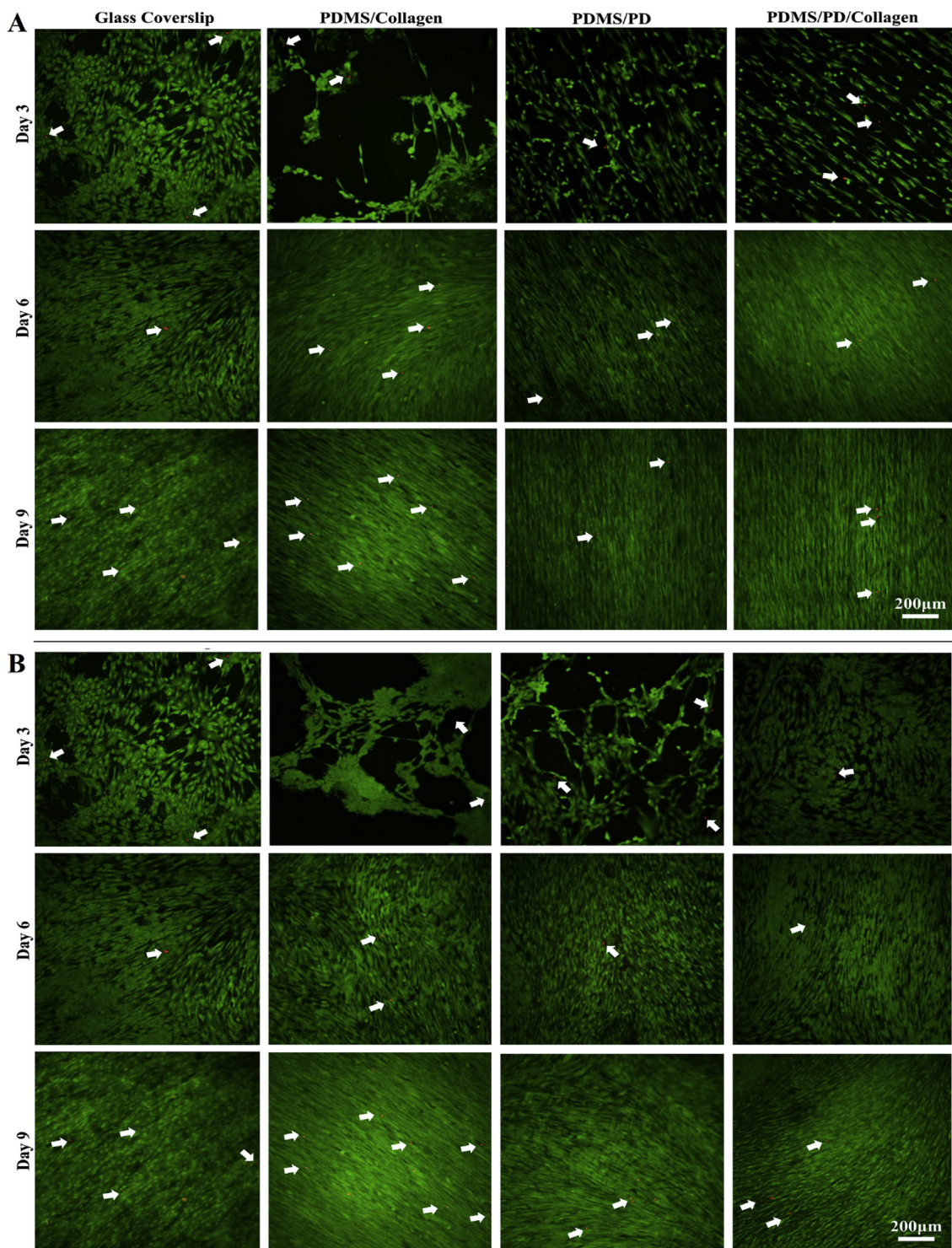


**Fig. 7.** Cytotoxicity analysis by live dead staining of hMSCs cultured on (A) aligned and (B) flat PDMS substrates. Viable hMSCs stained with Calcein AM gives green fluorescence. Dead cells containing EthD-1 gives red fluorescent signal due to compromised plasma membrane integrity (white arrows). No obvious difference in the dead cell signals was observed between control and different surface coatings.

Moreover, no significant difference in hMSCs coverage was observed between PDMS/PD and PDMS/PD/collagen surface treatment. Therefore, PDMS/PD coating can be solely applied for surface treatment. One of the preliminary studies that determined genotoxicity and cytotoxicity of PD on cancer and non-cancer cell lines proved that PD is biocompatible and does not promote significant genetic alteration in the cells [59]. Our cytotoxicity analysis from live/dead study further validated that PD and PD/collagen coatings do not promote significant

cytotoxicity, and therefore, are favorable for hMSC cultures (Fig. 7).

## 5. Conclusions

In this study, we have examined a PD-based and oxygen plasma-independent surface coating method for micro-grated PDMS substrates. The PD-based surface coatings can form a uniform layer on the micro-grafted PDMS substrates without affecting overall surface topography.

Moreover, PDMS/PD as well as PDMS/PD/collagen coatings significantly improved PDMS surface hydrophilicity and stiffness, which is essential for mammalian cell culture. The PD-based surface coating on PDMS substrates supported hMSC coverage and alignment without causing significant cytotoxicity. Results obtained from this study indicated that PD based surface coating is relatively simple, inexpensive and efficient for enhancing PDMS surface properties and can be useful for cell sheet cultures.

## Conflict of interest

No.

## Acknowledgements

This study was supported by the National Institutes of Health (1R15CA202656 and 1R15HL115521-01A1) and the National Science Foundation (1703570) to FZ.

## References

- [1] Q. Shen, et al., Adult SVZ stem cells lie in a vascular niche: a quantitative analysis of niche cell-cell interactions, *Cell Stem Cell* 3 (3) (2008) 289–300.
- [2] M. Tavazoie, et al., A specialized vascular niche for adult neural stem cells, *Cell Stem Cell* 3 (3) (2008) 279–288.
- [3] T. Yokomizo, E. Dzierzak, Three-dimensional cartography of hematopoietic clusters in the vasculature of whole mouse embryos, *Development* 137 (21) (2010) 3651–3661.
- [4] J.R. Anderson, et al., Exploring the retinal connectome, *Mol. Vis.* 17 (2011) 355–379.
- [5] F. Bosetti, et al., "Small blood vessels: big health problems?": scientific recommendations of the National Institutes of Health workshop, *J. Am. Heart Assoc.* 5 (11) (2016).
- [6] N. Kaneko, et al., Three-dimensional reconstruction of the human capillary network and the intramyocardial micronecrosis, *Am. J. Physiol. Heart Circ. Physiol.* 300 (3) (2011) H754–H761.
- [7] M.A. Nandkumar, et al., Two-dimensional cell sheet manipulation of heterotypically co-cultured lung cells utilizing temperature-responsive culture dishes results in long-term maintenance of differentiated epithelial cell functions, *Biomaterials* 23 (4) (2002) 1121–1130.
- [8] Q. Xing, et al., Highly aligned nanofibrous scaffold derived from decellularized human fibroblasts, *Adv. Funct. Mater.* 24 (20) (2014) 3027–3035.
- [9] N. Annabi, et al., Highly elastic micropatterned hydrogel for engineering functional cardiac tissue, *23* (39) (2013) 4950–4959.
- [10] W. Zhu, et al., Highly aligned nanocomposite scaffolds by electrospinning and electrospraying for neural tissue regeneration, *Nanomed. Nanotechnol. Biol. Med.* 11 (3) (2015) 693–704.
- [11] N.G. Rim, et al., Micropatterned cell sheets as structural building blocks for biomimetic vascular patches, *Biomaterials* 181 (2018) 126–139.
- [12] J. Hu, et al., Enhanced cell adhesion and alignment on micro-wavy patterned surfaces, *PLoS One* 9 (8) (2014) e104502.
- [13] A. Mata, A.J. Fleischman, S. Roy, Characterization of polydimethylsiloxane (PDMS) properties for biomedical micro/nanosystems, *Biomed. Microdevices* 7 (4) (2005) 281–293.
- [14] J.C. McDonald, G.M. Whitesides, Poly(dimethylsiloxane) as a material for fabricating microfluidic devices, *Acc. Chem. Res.* 35 (7) (2002) 491–499.
- [15] M. Nishikawa, et al., Stable Immobilization of Rat Hepatocytes as Hemispheroids onto Collagen-Conjugated Poly-Dimethylsiloxane (PDMS) Surfaces: Importance of Direct Oxygenation through PDMS for Both Formation and Function vol. 99, (2008), pp. 1472–1481 (6).
- [16] S.E. Woodcock, W.C. Johnson, Z. Chen, Collagen adsorption and structure on polymer surfaces observed by atomic force microscopy, *J. Colloid Interface Sci.* 292 (1) (2005) 99–107.
- [17] Z. Qian, et al., Bioactive polydimethylsiloxane surface for optimal human mesenchymal stem cell sheet culture, *Bioactive Mater.* 3 (2) (2018) 167–173.
- [18] H. Hillborg, et al., Crosslinked polydimethylsiloxane exposed to oxygen plasma studied by neutron reflectometry and other surface specific techniques, *Polymer* 41 (18) (2000) 6851–6863.
- [19] Y. Yang, et al., Effects of topographical and mechanical property alterations induced by oxygen plasma modification on stem cell behavior, *ACS Nano* 6 (10) (2012) 8591–8598.
- [20] H. Lee, et al., Mussel-inspired surface chemistry for multifunctional coatings, *Science* (New York, N.Y.) 318 (5849) (2007) 426–430.
- [21] P. Kord Forooshani, B.P. Lee, Recent approaches in designing bioadhesive materials inspired by mussel adhesive protein, *J. Polym. Sci. Polym. Chem.* 55 (1) (2017) 9–33.
- [22] Q. Wei, et al., Improving the blood compatibility of material surfaces via biomolecule-immobilized mussel-inspired coatings, *96A* (1) (2011) 38–45.
- [23] P. Xue, et al., Surface modification of poly(dimethylsiloxane) with polydopamine and hyaluronic acid to enhance hemocompatibility for potential applications in medical implants or devices, *ACS Appl. Mater. Interfaces* 9 (39) (2017) 33632–33644.
- [24] H. Lee, et al., Mussel-Inspired Surface Chemistry for Multifunctional Coatings, 318 (2007), pp. 426–430 (5849).
- [25] D.R. Dreyer, et al., Elucidating the structure of poly(dopamine), *Langmuir* 28 (15) (2012) 6428–6435.
- [26] B. Parekkadan, J.M. Milwid, Mesenchymal Stem Cells as Therapeutics vol. 12, (2010), pp. 87–117 (1).
- [27] L. Chen, et al., Pre-vascularization enhances therapeutic effects of human mesenchymal stem cell sheets in full thickness skin wound repair, *Theranostics* 7 (1) (2017) 117–131.
- [28] M.N. Knight, K.D. Hankenson, Mesenchymal stem cells in bone regeneration, *Adv. Wound Care* 2 (6) (2013) 306–316.
- [29] Z. Gong, L.E. Niklason, Small-diameter human vessel wall engineered from bone marrow-derived mesenchymal stem cells (hMSCs), *FASEB J.* : Off. Publ. Feder. Amer. Soc. Exper. Biol. 22 (6) (2008) 1635–1648.
- [30] Q. Xing, et al., Aligned nanofibrous cell-derived extracellular matrix for anisotropic vascular graft construction, 6 (10) (2017) 1601333.
- [31] D. Radke, et al., Tissue engineering at the blood-contacting surface: a review of challenges and strategies in vascular graft development, *Adv. Healthc. Mater.* 7 (15) (2018) e1701461.
- [32] S. Roura, et al., Mesenchymal stem cells for cardiac repair: are the actors ready for the clinical scenario? *Stem Cell Res. Ther.* 8 (1) (2017) 238–238.
- [33] S. Bahsoon, et al., The role of dissolved oxygen levels on human mesenchymal stem cell culture success, regulatory compliance, and therapeutic potential, *Stem Cell Dev.* 27 (19) (2018) 1303–1321.
- [34] L. Zhang, et al., Hypoxia created human mesenchymal stem cell sheet for pre-vascularized 3D tissue construction, *Adv. Healthc. Mater.* 5 (3) (2016) 342–352.
- [35] D. Sharma, J. Chica, F. Zhao, Mesenchymal Stem Cells for Pre-vascularization of Engineered Tissues, (2018).
- [36] F. Zhao, et al., Low oxygen tension and synthetic nanogratings improve the uniformity and stemness of human mesenchymal stem cell layer, *Mol. Ther.* 18 (5) (2010) 1010–1018.
- [37] Y.J. Chuah, et al., Simple surface engineering of polydimethylsiloxane with poly-dopamine for stabilized mesenchymal stem cell adhesion and multipotency, *Sci. Rep.* 5 (2015) 18162.
- [38] J.E. Sader, et al., Spring constant calibration of atomic force microscope cantilevers of arbitrary shape, *Rev. Sci. Instrum.* 83 (10) (2012) 103705.
- [39] S.J. Martin, V.E. Granstaff, G.C. Frye, Characterization of a quartz crystal microbalance with simultaneous mass and liquid loading, *Anal. Chem.* 63 (20) (1991) 2272–2281.
- [40] H. Lee, J. Rho, P.B. Messersmith, Facile conjugation of biomolecules onto surfaces via mussel adhesive protein inspired coatings, 21 (4) (2009) 431–434.
- [41] I. You, et al., Fabrication of a micro-omnifluidic device by omniphilic/omniphobic patterning on nanostructured surfaces, *ACS Nano* 8 (9) (2014) 9016–9024.
- [42] L.M. Johnson, et al., Elastomeric microparticles for acoustic mediated bioseparations, *J. Nanobiotechnol.* 11 (2013) 22.
- [43] M. Zhang, et al., The rheological and structural properties of fish collagen cross-linked by N-hydroxysuccinimide activated adipic acid, *Food Hydrocolloids* 30 (2) (2013) 504–511.
- [44] B. de Campos Vidal, M.L.S. Mello, Collagen type I amide I band infrared spectroscopy, *Micron* 42 (3) (2011) 283–289.
- [45] H. Luo, et al., Facile synthesis of novel size-controlled antibacterial hybrid spheres using silver nanoparticles loaded with poly-dopamine spheres, *RSC Adv.* 5 (18) (2015) 13470–13477.
- [46] P. Yan, et al., The in vitro biomineratization and cytocompatibility of polydopamine coated carbon nanotubes, *Appl. Surf. Sci.* 257 (11) (2011) 4849–4855.
- [47] W. Sheng, et al., Brushing up from "anywhere" under sunlight: a universal surface-initiated polymerization from polydopamine-coated surfaces, *Chem. Sci.* 6 (3) (2015) 2068–2073.
- [48] S. Zhu, et al., Fabrication of a novel bio-inspired collagen–polydopamine hydrogel and insights into the formation mechanism for biomedical applications, *RSC Adv.* 6 (70) (2016) 66180–66190.
- [49] S.E. Woodcock, W.C. Johnson, Z. Chen, Collagen adsorption and structure on polymer surfaces observed by atomic force microscopy, *J. Colloid Interface Sci.* 292 (1) (2005) 99–107.
- [50] M. Fang, et al., A facile approach to construct hierarchical dense membranes via polydopamine for enhanced propylene/nitrogen separation, *J. Membr. Sci.* 499 (2016) 290–300.
- [51] C.Y. Kuan, a.M.H. H, a.J.M. Chou b, I.C. Leu, Wetting characteristics on micro/nanostructured zinc oxide coatings, *J. Electrochem. Soc.* 156 (2009) 32–36.
- [52] D. Kang, et al., Mechanical Properties of Poly(dopamine)-coated Graphene oxide and Poly(vinyl alcohol) Composite Fibers Coated with Reduced Graphene oxide and their Use for Piezoresistive Sensing vol. 34, (2017), p. 1600382 (9).
- [53] F.K. Yang, et al., "Contact" of nanoscale stiff films, *Langmuir* 28 (25) (2012) 9562–9572.
- [54] X. Hu, et al., The influence of elasticity and surface roughness on myogenic and osteogenic differentiation of cells on silk-elastin biomaterials, *Biomaterials* 32 (34) (2011) 8979–8989.
- [55] N.D. Evans, et al., Substrate stiffness affects early differentiation events in embryonic stem cells, *Eur. Cells Mater.* 18 (2009) 1–13 discussion 13–4.
- [56] J.T. Pham, et al., Guiding cell migration with microscale stiffness patterns and undulated surfaces, *Acta Biomater.* 38 (2016) 106–115.
- [57] Y. Kim, C. Kwon, H. Jeon, Genetically engineered phage induced selective H9c2 cardiomyocytes patterning in PDMS microgrooves, *Materials* 10 (8) (2017).
- [58] G. Fu, W.O. Soboyejo, Cell/surface interactions of human osteo-sarcoma (HOS) cells and micro-patterned polydimethylsiloxane (PDMS) surfaces, *Mater. Sci. Eng. C* 29 (6) (2009) 2011–2018.
- [59] A. Woźniak, et al., In vitro genotoxicity and cytotoxicity of polydopamine-coated magnetic nanostructures, *Toxicol. Vitro* 44 (2017) 256–265.